Original Article
MiR-378 overexpression attenuates high glucose-suppressed osteogenic differentiation through targeting CASP3 and activating PI3K/Akt signaling pathway

Li You, Wensha Gu, Lin Chen, Ling Pan, Jinyu Chen, Yongde Peng

Department of Endocrinology and Metabolism, Shanghai First People's Hospital, Shanghai Jiao Tong University School of Medicine, 100 Haining Road, Shanghai 200080, China

Abstract: Hyperglycemia is one of the possible causes for osteoporosis and bone fracture in diabetes mellitus. Here we modeled diabetes-induced osteoporosis *in vitro* using preosteoblastic cell line MC3T3-E1 and a diabetic mice model for *in vivo* studies. We found that in addition to reducing osteoblast viability and differentiation (mineralization), culture in elevated glucose down regulated microRNA-378 (miR-378) expression but ectopic miR-378 expression reversed the effects of high glucose. We identified caspase-3 (CASP3) as a target of miR-378 and showed that miR-378 repressed CASP3 mRNA and protein expression under high glucose condition. We further showed that both miR-378 expression and CASP3 silencing independently restored alkaline phosphatase (ALP) activity and the expression of osteoblastic differentiation markers Runt-related transcription factor 2 (Runx2), osteorix (Osx), collagen I (Col I), osteocalcin (OCN), and osteonectin (ON). We also found that under high glucose conditions miR-378 activated the PI3K/Akt signaling pathway and down regulated pro-apoptotic CytC, Apaf-1 and Bax proteins via the PI3K/Akt pathway. Collectively, these results suggest that miR-378 overexpression attenuates high glucose-suppressed osteogenic differentiation through targeting CASP3 and activating the PI3K/Akt pathway.

Keywords: MiR-378, high glucose, CASP3, osteogenic differentiation, PI3K/Akt signaling

Introduction

Diabetes mellitus is a chronic metabolic disorder characterized by high blood glucose levels resulting from defects in insulin secretion (type 1 diabetes), insulin action (type 2 diabetes), or both. One of the many organs affected by diabetes mellitus is bone. Type 1 diabetes may result in diabetic osteoporosis whereas type 2 diabetes mellitus is more commonly associated with modest increases in bone mineral density. Despite this dichotomy, a growing body of evidence supports the fact that the diabetic state disturbs the formation of new bone as well as the integrity of bone microarchitecture, and thus bone quality, leading to an increased risk for fragility fracture and inadequate bone regeneration following injury [1].

Increasing evidence suggests that hyperglycemia plays a role in the pathogenesis of diabetic bone disease. Bone homeostasis is maintained through a balance between bone resorption by osteoclasts followed by bone formation by osteoblasts. The primary cause for altered bone metabolism in diabetes appears to be a decrease in the activity of the osteoblast [2, 3]. In both animal models and humans with hyperglycemia, a decrease in osteoblast activity has been reported [4]. Because the serum of diabetic patients not only shows an elevated glucose concentration, but also alterations in insulin or other hormones, free fatty acid, and ketone bodies, all of which could impact osteoblast activity, cellular models are a useful *in vitro* tool to study the effects of single components associated with diabetes. The culture of osteoblasts in high glucose concentrations affects both the capacity for osteoblastic differentiation as well as cell viability. However, the published literature reveals contradictory effects of hyperglycemia on the mineralization pro-

cess in the different studies, some reporting decreased mineralization [5-8] and others an increased mineralization [9, 10], which may be due to the differences in experimental conditions, heterogeneous cell sources and different glucose concentrations used.

Osteoblast differentiation involves a series of stages, including proliferation, matrix development and matrix mineralization. At the molecular level, osteoblast differentiation and bone formation is driven by signaling molecules including PI3K/Akt [11], Hedgehog [12, 13], TGF-β/BMP [14-17], Wnt/beta-catenin [18] and p38 family members [19] and transcription factors including Runt-related transcription factor (Runx2) [20], osteorix (Osx) [21], osteocalcin (OCN) [22] and osteonectin (ON) [23]. Although high glucose suppresses matrix mineralization in mouse osteoblasts MC3T3-E1, the precise stages and differentiation programs affected by hyper physiological glucose remain unclear. High glucose has been shown to inhibit osteogenic differentiation by activating the cAMP/PKA/ERK pathway [24], inhibiting the Wnt signaling pathway [25] and up regulating c-Jun [26]. High glucose induces apoptosis in MC3T3-E1 by activating p38MAPK signaling, which when reduced by microRNA (miRNA) targeting reverses the apoptotic effect of high glucose [27].

MiRNAs function as gene silencers and are emerging as important regulators of gene expression and biological processes. As opposed to transcription factors, which initiate gene expression, miRNAs normally repress gene expression. MiRNAs are single-stranded RNA of ~22-nt in length that post transcriptionally silence target genes by partially complementing with the 3' untranslated region (UTR) of target mRNA. MiRNAs play key roles in diverse regulatory pathways, including development, cell differentiation, apoptosis and cell proliferation. Multiple miRNAs play a role in the sequential steps of osteogenesis [28, 29]. Recently it was found that miR-378 suppresses osteoblast differentiation by down regulating UDP-N-acetyl-α-D-galactosamine: polypeptide N-acetylgalactosaminyltransferase 7 (GalNT-7), an enzyme known to glycosylate proteins, including osteogenesis enhancer nephronectin [30]. MiR-378 was also involved in the induction of osteoclast differentiation in mesenchymal progenitor cells [31]. MiR-378 was originally identified as

an oncogene promoting VEGF expression in human nasopharyngeal carcinoma cell line CNE [32]. The ability to silence caspase-3 (CASP3) in cultured glioma cells [33] and cardiac myocytes [34] establishes miR-378 as a suppressor of apoptosis.

In this study, the role of miR-378 in osteoblast response to high glucose was evaluated through measurement of cell viability, apoptosis, mineralization analysis and alkaline phosphatase (ALP) activity after ectopic expression of miR-378. The target of miR-378, CASP3, was identified, as well as the effect of CASP3 inhibition on osteoblast differentiation capacity in high glucose conditions. Akt was a physiological substrate of CASP3 [35], And PI3K/Akt pathway was involved in the osteogenic differentiation of MC3T3-E1 cells [11]. PI3K/Akt pathway and related pro-apoptotic protein expressions were also determined *in vitro* and *in vivo* to explore the underlying molecular mechanism.

Materials and methods

Cell culture

Mouse osteoblastic cell line MC3T3-E1 (American Type Culture Collection, USA) was plated at a density of 10^5 cells/cm^2 and incubated in α-MEM (containing 5.5 mM glucose) supplemented with 10% FBS, 100 U/mL penicillin and 100 U/mL streptomycin, 37°C, 5% CO_2 with a media change every 2-3 days. At 80% confluence MC3T3-E1 cells were cultured in α-MEM containing normal glucose (5.5 mM) or high glucose (15.5, 25.5 or 35.5 mM) for selected time periods. For signal pathway studies, cells under high glucose (25.5 mM) were treated with 20 μM PI3K inhibitor, LY294002 (Selleck, USA) for the indicated time.

Lentivirus production and cell transfection

MCT3T3-E1 cells stably expressing miR-378 (MC3T3-E1/miR-378) or miR-con (MC3T3-E1/miR-con) were generated as follows. The lentiviral vector was prepared following a standard protocol using the pre-miR-378 encoding sequence subcloned into transfer vector pCDH-CMV-MCS-EF1-copGFP. Empty vector was used as the control. Virus packaging was performed in HEK 293T cells after cotransfection of pCDH-miR-378 vector or pCDH-miR-control with the

packaging plasmid psPAX2 and envelope plasmid pMD2.G (Tronolab, Switzerland) using Lipofectamine 2000 (Invitrogen, USA). After 72 h, lentivirus in the supernatant was harvested and polybrene was added to the final concentration 8 μg/mL. Lentivirus was transduced into MC3T3-E1 cells with Polybrene (Sigma, USA). The transduced cells were collected 48 h post-infection for further experiments. For CASP3 silencing, CASP3 short hairpin RNA (shRNA) was designed (5'-CGC GTC CCC TGA CAT CTC GGT CTG GTA CTT CAA GAG ATA CCA GTG GAG GCC GAC TTT TTT TGG AAA T-3') and inserted into pLVTHM plasmid (Tronolab, Switzerland). Virus packaging and cell transfection were performed as described before [36].

Cell viability assay

Cell viability was measured using a colorimetric assay based on the ability of viable cells to convert soluble 3-(4,5-dimethyl-thiazol-2yl)-2,5-diphenyl tetrazolium bromide (MTT; Sigma, USA) into an insoluble dark blue formazan reaction product. Briefly, cells plated in 96-well plates were treated with 5 mg/mL MTT solution for 4 h. Dimethyl sulfoxide (Sigma, USA) was added to all wells and mixed thoroughly to dissolve the dark blue crystals. Plates were read at 570 nm on a microplate reader. Every experiment was repeated three times.

Cell apoptosis analysis

Cell apoptosis was examined by flow cytometry through Annexin V-FITC/Propidium Iodide (PI) double staining assay. MC3T3-E1 cells were harvested, washed with cold phosphate buffered saline (PBS) and suspended in binding buffer containing 10 mM HEPES/NaOH (pH 7.4), 140 mM NaCl, 2.5 mM $CaCl_2$ at a concentration of 10^6 cells/mL. Then the cells were stained with Annexin V-FITC and PI followed and analyzed on the flow cytometer to evaluate the percentage of apoptotic cells. Experiment was repeated three times and data were analyzed with Cell Quest Software.

Analysis of mineralization

The extent of mineralization was determined after 21 days by Alizarin Red S staining, which detects calcium deposition [37]. After rinsing in phosphate buffered saline and fixing in 70% ice-cold ethanol, the cells were stained with 40 mM Alizarin Red S (pH 4.2; Sigma, USA) for 20 min at room temperature. To quantify calcium content, the amount of Alizarin Red S bound to mineralizing nodules was measured as follows. After staining, cultures were briefly washed in PBS and extracted with 10% (w/v) cetylpyridinium chloride (Sigma, USA) in 10 mM sodium phosphate pH 7.0 for 10 min at RT. Dye concentration was determined by measuring the absorbance at 550 nm. Each experiment was conducted three times.

Measurement of ALP activity

ALP activity was measured by the colorimetric conversion of p-nitrophenyl phosphate to p-nitrophenol using reagents from an ALP assay Kit (WAKO, Japan) according to manufacture's instruction [38]. MC3T3-E1 cells seeded in triplicate at $10^5/cm^2$ in a 6-well culture plate were left to attach for 24 h. Cells were then treated with 25.5 mM glucose for 14 days after which the cells were collected and lysed by ultrasound at 4°C. Protein concentration was measured with the Bradford Assay (Bio-Rad, CA). The absorbance of lysates was measured with a microplate reader at 405 nm. ALP activity was calculated using p-nitrophenol as standard and denoted as nmol/min/μg protein. Experiment was repeated three times.

Quantitative real-time polymerase chain reaction (qRT-PCR)

RNA was extracted with Trizol (Invitrogen, USA), and the content was assessed by 260 nm absorbance and the sample's purity was assessed by the A260/A280 ratio. Total RNA was reverse transcribed (GoScript™ Reverse Transcriptase, Promega, Beijing) and cDNA was stored at -20°C at 10 ng/μL in nuclease-free water. qRT-PCRs were performed using the SYBR-Green detection method and run on Light Cycling 480 (Roche, Switzerland). All primers were synthesized by Sangon Biotech (Shanghai). Reactions were run in triplicate and normalized to the corresponding internal standard controls. Primer sequences for miR-378, reverse transcription primer, 5'-CTC AAC TGG TGT CGT GGA GTC GGC AAT TCA GTT GAG GCC TTC TG-3', forward, 5'-GCA CTG GAC TTG GAG TC-3' and reverse, 5'-GTG CAG GGT CGA GGT-3'; and the internal control snRNA U6, forward, 5'-CTC GCT TCG GCA GCA CA-3' and reverse, 5'-AAC GCT TCA CGA ATT TGC GT-3'. Primer sequences for

Table 1. Primer sequence used for real-time RT-PCR. The primer sequences for target and reference genes, product size and accession number are shown

Name		5'-Sequence-3'	Product size	Accession number
CASP3	F	TGGAACAAATGGACCTGTTGACC	365 bp	NM_009810
	R	AGGACTCAAATTCTGTTGCCACC		
Runx2	F	GTGGCCTTCAAGGTTGTAG	326 bp	XM_006523547
	R	GGGTAAGACTGGTCATAGG		
Osx	F	CCCTTCTCAAGCACCAATG	500 bp	XM_006520520
	R	GCCTTGGGCTTATAGACATC		
Col I	F	CAGGCTGGTGTGATGGGATT	317 bp	NM_007742
	R	AAACCTCTCTCGCCTCTTGC		
OCN	F	TCTGACAAAGCCTTCATGTCC	199 bp	NM_031368
	R	AAATAGTGATACCGTAGATGCG		
ON	F	CTGCTCGCCTCTAAACCC	321 bp	NM_009242
	R	TTGTCAGCCACCACCTCC		
β-actin	F	TATGCTCTCCCTCACGCCA	369 bp	NM_007393
	R	TTTACGGATGTCAACGTCACAC		

genes were listed in **Table 1**. All samples were analyzed in triplicate.

Western blot analysis

Cells were rinsed in ice-cold PBS and then homogenized in RIPA buffer (Santa Cruz Biotechnology, USA). Homogenates were centrifuged at 12,000 rpm for 20 min at 4°C. Protein concentrations were measured with a BCA-assay kit (Pierce, USA). 10 μg proteins were separated by sodium dodecyl sulfate polyacrylamide gel electrophoresis (SDS-PAGE), and then electro-transferred to Hybond-polyvinylidenefluoride membrane followed by blocking and incubation with primary antibodies (anti-CASP3, anti-β-actin, anti-p-PI3K, anti-PI3K, anti-p-Akt, anti-Akt, anti-Cyt C, anti-Apaf-1 and Bax; Abcam, UK) at 4°C overnight. After washing with Tris-buffered saline with Tween 20 (TBST), membranes were incubated in TBST containing horseradish peroxidase conjugated goat anti-rabbit IgG antibody (Abcam, UK) at room temperature for 2 h followed by ECL detection. All samples were analyzed in duplicate.

Luciferase reporter assay

The 3' untranslated region (3'UTR) sequence of CASP3, containing the putative miR-378 binding site or the mutated one, was cloned into the region directly down-stream of the stop codon in the luciferase gene in luciferase reporter vector, which was named pGL3-CASP3-3'UTR (wt) or pGL3-CASP3-3'UTR (mut). MC3T3-E1

cells stably expressing miR-378 or miR control were cotransfected with pGL3-CASP3-3'UTR (wt) or pGL3-CASP3-3'UTR (mut) reporter vector together with pRL-TK using Lipofectamine 2000 (Invitrogen) according to the manufacturer's protocol. Cells were lysed 24 h after transfection, and luciferase activities were measured using the Dual-Luciferase® Reporter Assay System (Promega). The Renilla-signal was used for normalization. Mean values and S.E.M. were calculated in triplicates.

In vivo studies

Thirty male mice (8-week-old, 37.82 ± 1.26 g) were divided into normal control group (NG group, n = 6) and diabetic model group (HG group, n = 24). The diabetic model mice were induced by intravenous administration of streptozotocin (Sigma, USA) at a dose of 50 mg/kg/day for 5 consecutive days [39-41]. Blood glucose level was measured one week after the induction, and mice with glucose concentration greater than 16.7 mM were defined as diabetic model mice. Sixteen diabetic mice were randomized into 2 groups (n = 8 per group) and mice were injected intraperitoneally with lentiviral vectors expressing miR-con or miR-378 (10^7 transducing units in 100 μL PBS per mouse) to study the function of miR-378 under hyperglycemic condition [42]. Whole tibia was homogenized into powder and lysed for gene expression analysis according to the method described before [43].

Statistical analysis

All experiments were performed in triplicate. Statistical analyses were performed using the Student's t test. P < 0.05 was considered to be significant.

Results

Effect of glucose on osteoblast differentiation and viability

To test the effect of hyper physiological glucose on the mineralization process of osteoblastic
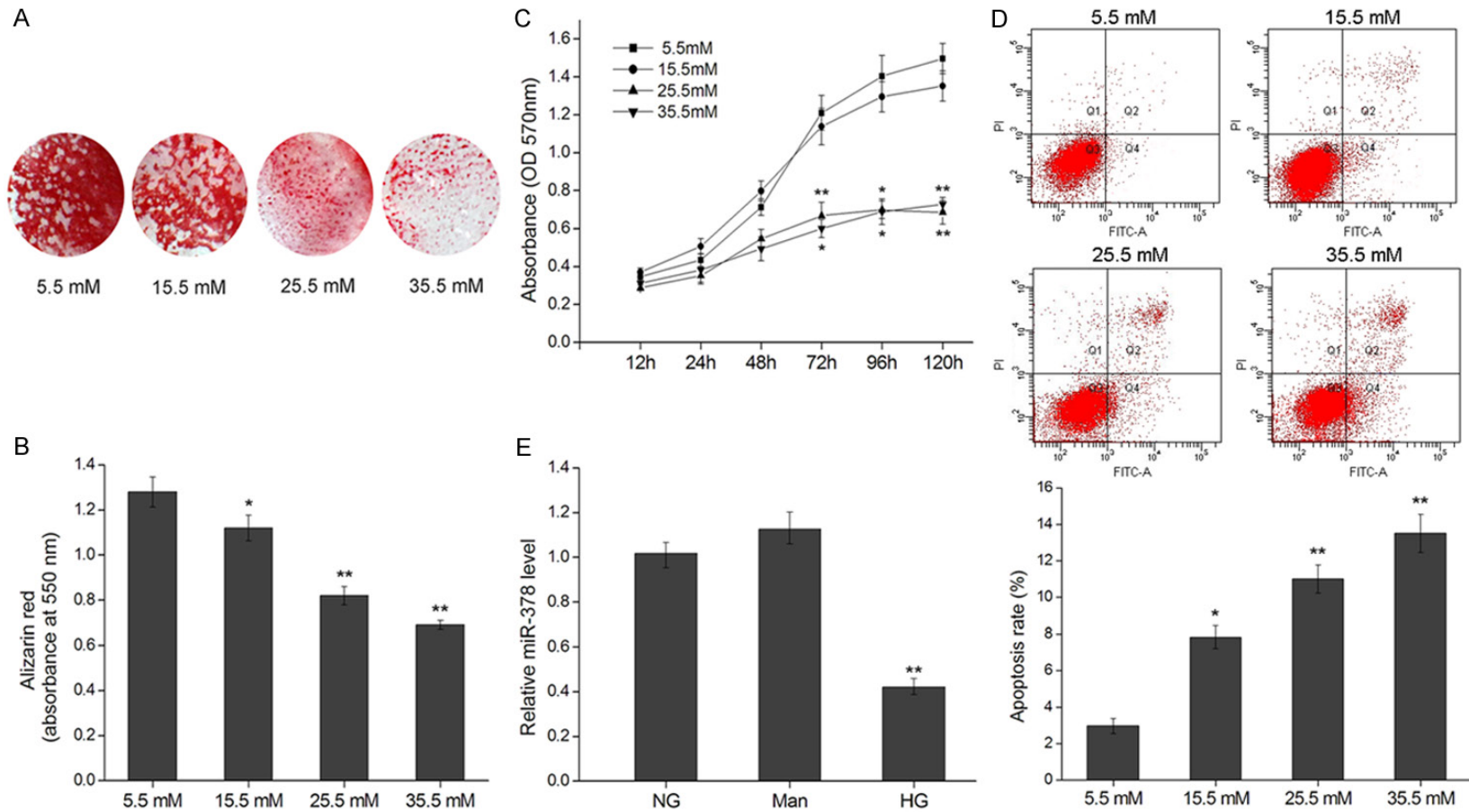
Figure 1. High glucose inhibits cell growth and mineralization of MC3T3-E1 and down regulates miR-378. A. Mineralization of osteoblasts cultured in glucose (5.5-35.5 mM) for 21 d depicted by Alizarin Red S staining. B. Alizarin Red S quantification by absorbance (at 550 nm) of osteoblasts cultured in Glucose (5.5-35.5 mM) for 21 d. C. Viability of osteoblasts cultured in glucose (5.5-35.5 mM) for 12-120 h represented by production of formazan in an MTT assay. D. Cell apoptosis of MC3T3-E1 cells after incubation with the indicated concentration of glucose for 120 h was evaluated by flow cytometry using Annexin V/PI-double staining. The apoptosis rates were the values of Q2 quadrant (Annexin V+/PI+) plus Q4 quadrant (Annexin V+/PI-). E. Relative miR-378 levels assayed by qRT-PCR in MC3T3-E1 cells cultured in no glucose (NG), mannose (Man) or high glucose (HG, 25.5 mM) for 120 h. *$P < 0.05$, **$P < 0.01$.
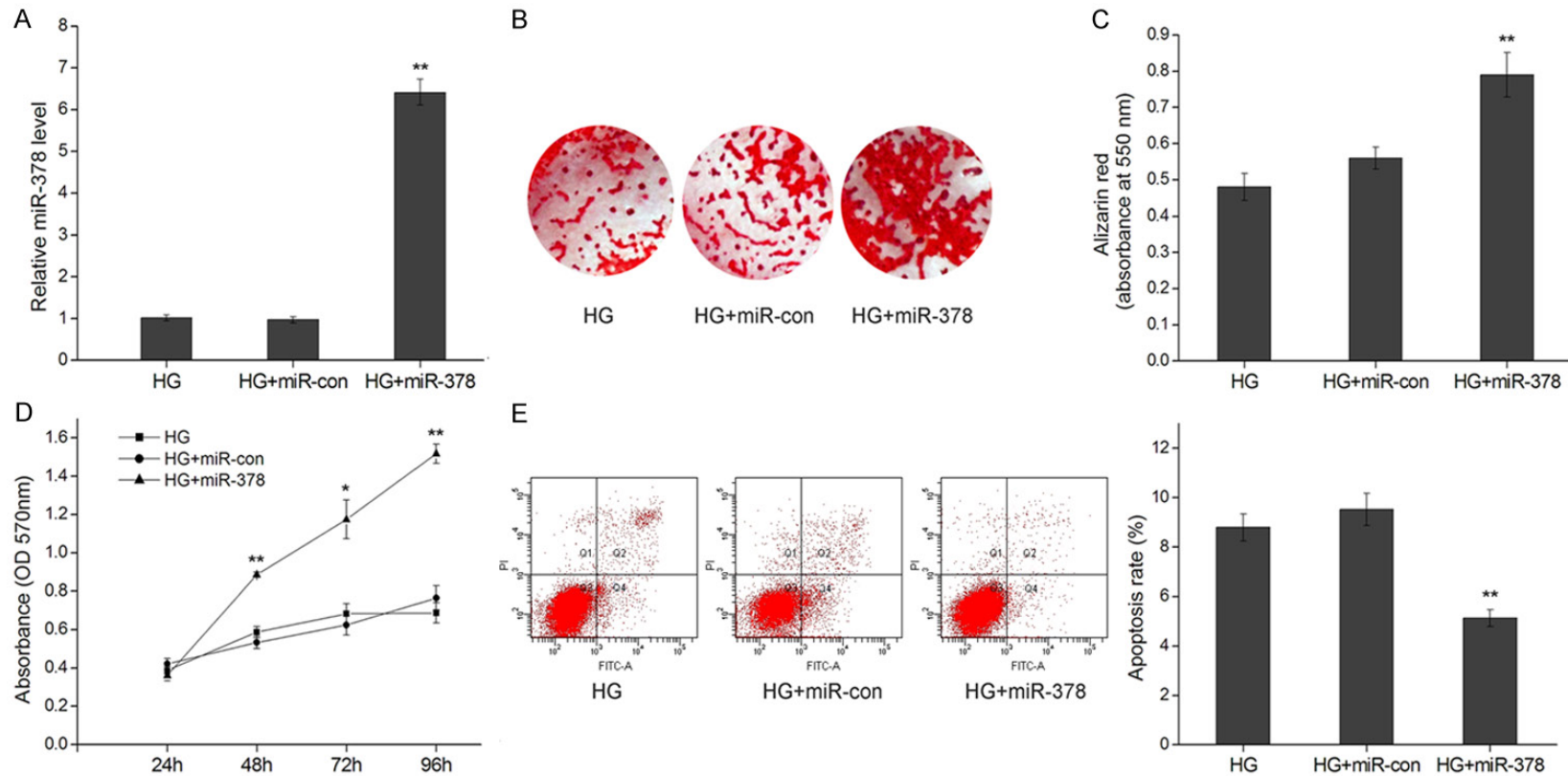
Figure 2. MiR-378 overexpression improves cell viability and mineralization under high glucose. A. Relative qRT-PCR expression levels of miR-378 48 h after transfection in MC3T3-E1, MC3T3-E1/miR-con and MC3T3-E1/miR-378 cells under high glucose (HG, 25.5 mM). B. Mineralization of osteoblasts cultured in HG for 21 d depicted by Alizarin Red S staining. C. Alizarin Red S quantification by absorbance (at 550 nm) of osteoblasts cultured in HG for 21 d. D. Viability of MC3T3-E1, MC3T3-E1/miR-con and MC3T3-E1/miR-378 cells cultured in HG for 24-96 h represented by production of formazan in an MTT assay. E. Representative flow cytometric analysis of apoptosis in MC3T3-E1 cells 48 h after transfection. The apoptosis rates were the values of Q2 quadrant plus Q4 quadrant. $^*P < 0.05$, $^{**}P < 0.01$.
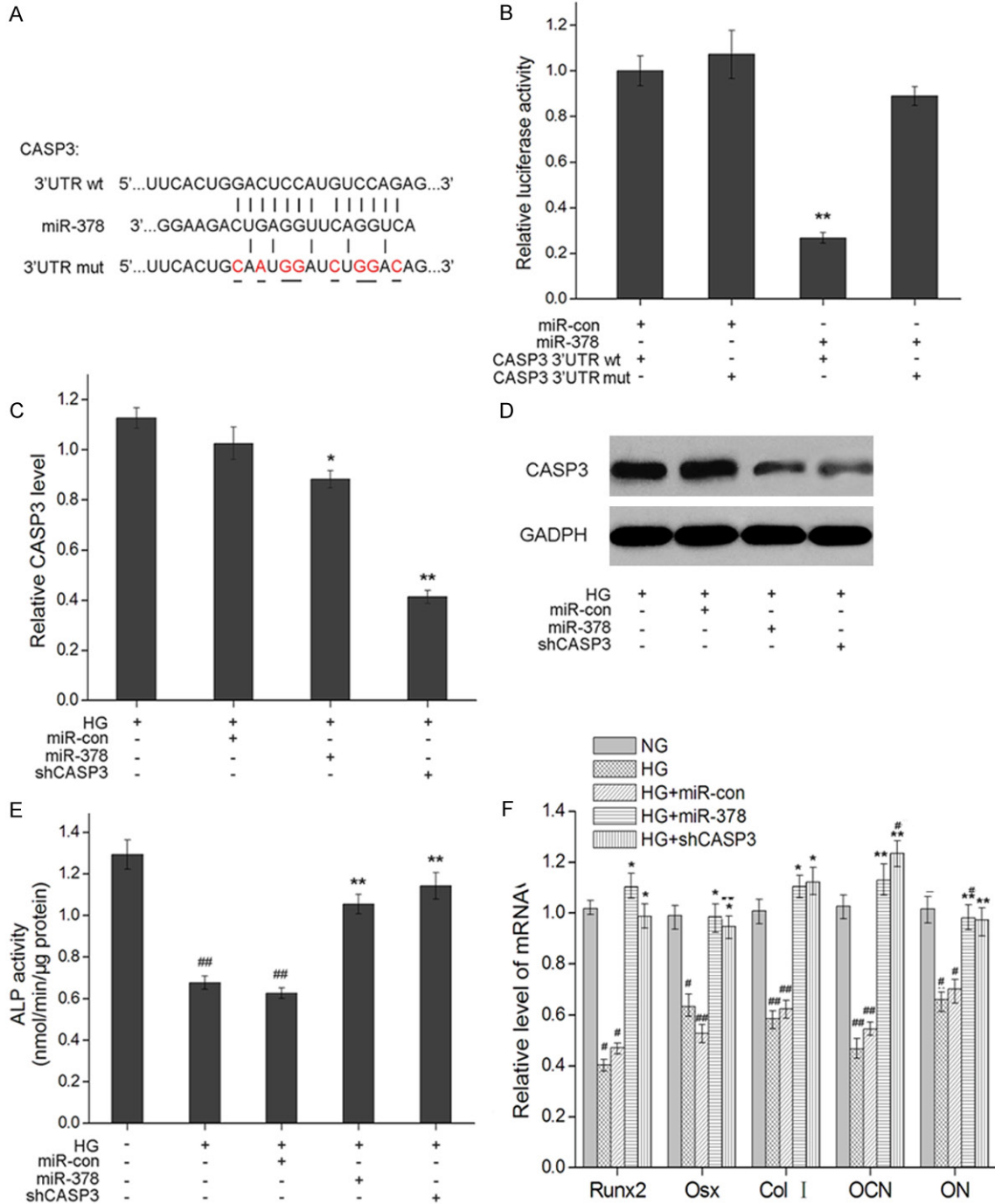
Figure 3. MiR-378 post transcriptionally down-regulates CASP3 expression by targeting its 3'UTR. A. Sequence complementarity between mmu-miR-378 and the seed region in the CASP3 3'UTR. Base pair mutations in the mutation-bearing construct are underlined. Short vertical lines indicate complementary nucleotides. B. Relative luciferase activity in MC3T3-E1 cells cultured in high glucose (HG, 25 mM) 24 h after co-transfection of miR-378 (Ambion) or mock vector (miR-con) with wild-type (wt) or mutant (mut) CASP3 3'UTR-luciferase reporter vector. Measurements from three biological replicates for each combination of constructs are shown along with SEM and **indicate $P <$ 0.01. C. CASP3 mRNA expression levels 48 h after transfection in MC3T3-E1, MC3T3-E1/miR-con and MC3T3-E1/miR-378 and MC3T3-E1/shCASP3 cells cultured in HG. Relative mRNA expression was detected by qRT-RCR. GADPH was used as an internal control. D. Western blot assays of CASP3 protein levels 48 h after transfection in MC3T3-E1, MC3T3-E1/miR-con and MC3T3-E1/miR-378 and MC3T3-E1/shCASP3 cells cultured under HG. E. ALP activity of MC3T3-E1, MC3T3-E1/miR-con and MC3T3-E1/miR-378 and MC3T3-E1/shCASP3 cells cultured in high glucose (25.5 mM) for 14 days. $^{*}P <$ 0.05 and $^{**}P <$ 0.01 compared to MC3T3-E1 cells cultured in HG; $^{#}P <$ 0.05

and ##$P < 0.01$ compared to MC3T3-E1 cells cultured in 5.5 mM glucose. F. mRNA expression levels of osteogenic marker genes in MC3T3-E1, MC3T3-E1/miR-con, MC3T3-E1/miR-378 and MC3T3-E1/shCASP3 cells cultured in HG for 2 days *$P < 0.05$ and **$P < 0.01$ compared with MC3T3-E1 in HG; #$P < 0.05$ and ##$P < 0.01$ compared with MC3T3-E1 cells in physiological levels of glucose (NG).
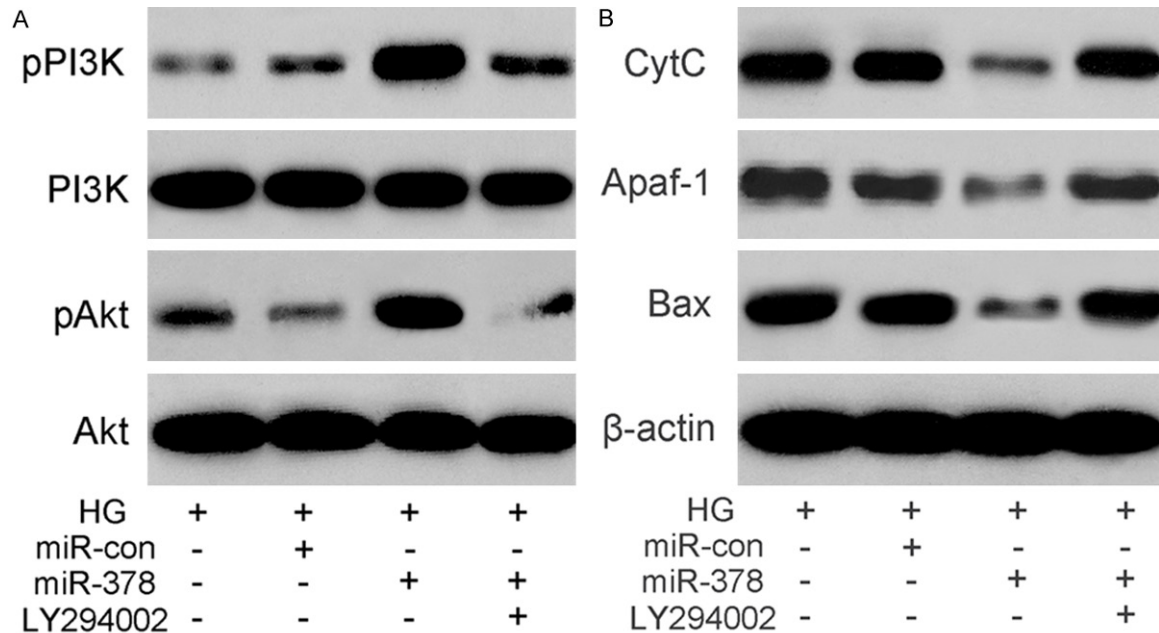

Figure 4. MiR-378 down regulates expression of apoptosis-related proteins through the activation of the PI3K/Akt pathway. (A) The expression of p-PI3K, p-Akt and (B) apoptosis proteins Cyt C, Apaf-1, and Bax detected by western blotting of protein samples from high glucose (25.5 mM) cultures of MC3T3-E1/miR-378 cells treated (+) or not treated (-) with PI3K inhibitor LY294002. β-actin was an internal control.

cells, MC3T3-E1 cells were cultured in 5.5-35.5 mM glucose for 21 d after which the presence of mineralized calcium deposit was characterized using the Alizarin Red S dye. Cells incubated at physiological levels of glucose (5.5 mM) showed extensive matrix calcification characterized by a high proportion of stained matrix (**Figure 1A**). However, cells cultured in non-physiological glucose concentrations showed decreased matrix calcification characterized by a decreased Alizarin Red S dye-positive matrix. In addition to this quantitative analysis, the amount of calcium was quantified using an absorbance-based assay (**Figure 1B**). The amount of calcium was significantly decreased when cells were cultured in all higher concentrations of glucose (15.5-35.5 mM). To determine whether hyper physiological glucose levels decreased cell viability, we cultured osteoblasts in 5.5-35.5 mM glucose for 5 d and subsequently determined cell viability at time points between 12-120 h. After 3 d in culture, osteoblasts in 25.5 and 35.5 mM glucose displayed reduced viability compared to 15.5 mM

and physiological glucose (**Figure 1C**). Besides, cell apoptosis rate was significantly increased when cells were cultured in higher concentrations of glucose (15.5-35.5 mM), which confirmed the effect of high glucose on cell viability (**Figure 1D**).

High glucose concentrations repress miR-378 expression

To probe the function of miR-378 in osteoblast response to glucose, we determined the levels of miR-378 in osteoblasts cultured in physiological and high glucose (25.5 mM) for 5 d alongside those cultured in mannitol, to control for the effects of osmosis, as higher levels of glucose may suppress osteogenic development as a result of changes in osmolarity [44]. We found that miR-378 was significantly down regulated in osteoblasts cultured in high glucose (**Figure 1E**). This suggests that the suppression of osteoblast viability and differentiation by high glucose may be a result of a miR-378 down regulation and its downstream effects.
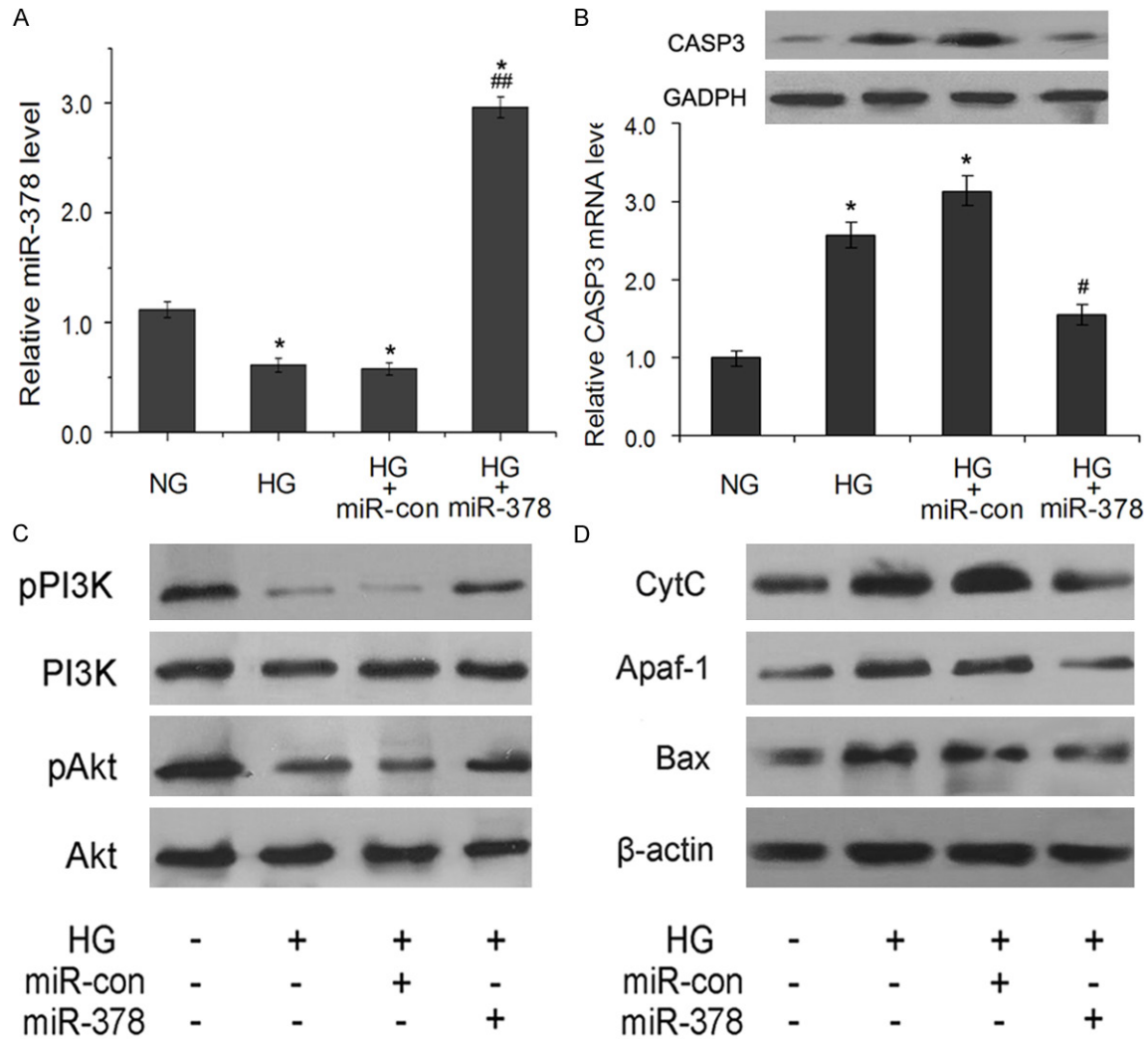
Figure 5. MiR-378 regulates expression of CASP3 and PI3K/Akt pathway in diabetic model mice. (A) Relative expression levels of miR-378 in tibias of normal and diabetic mice injected with miR-con (HG+miR-con group) or miR-378 (HG+miR-378 group). (B) Relative mRNA and protein expressions of CASP3 in rat tibias. (C) The expression of p-PI3K, p-Akt and apoptosis proteins Cyt C, Apaf-1, and Bax (D) detected by western blotting of protein samples from tibias of normal and diabetic mice injected with miR-con or miR-378. β-actin was an internal control. $^*P < 0.05$ compared with normal mice (NG group); $\#P < 0.05$ and $\#\#P < 0.01$ compared with diabetic mice (HG group).

Ectopic miR-378 enhances osteogenic differentiation

We next explored the function of miR-378 in osteoblast differentiation by stably expressing miR-378 by lentiviral integration in MC3T3-E1 cells (**Figure 2A**). After differentiation in 25.5 mM glucose for 21 d, MC3T3-E1 cells stably expressing miR-378 (MC3T3-E1/miR-378) displayed an increased proportion of stained matrix as characterized by Alizarin Red S dye staining (**Figure 2B**), and when measured quantitatively, a significantly increased amount of calcium (**Figure 2C**) compared to MC3T3-E1

cells alone or those stably expressing the control vector (MC3T3-E1/miR-con). In addition, miR-378 expression restored cell viability (**Figure 2D**) and reduced cell apoptosis (**Figure 2E**).

MiR-378 targets the CASP3 3'UTR

To explore the mechanism by which miR-378 reverses glucose-suppressed viability and differentiation, we focused on its known target CASP3 [33, 34]. To confirm the target sequence of miR-378 in the 3'UTR of CASP3 (**Figure 3A**) in osteoblasts, we integrated a fragment of the

CASP3 3'UTR containing the target sequence, or the fragment whose target sequence was mutated (**Figure 3A**), into a luciferase reporter vector. When co-transfected with miR-378 or its negative control miR-con into MC3T3-E1 cells, luciferase activity was significantly repressed in the construct harboring the wild type sequence compared with the control vector or the vector harboring the mutated sequence (**Figure 3B**), confirming CASP3 as a miR-378 target. MiRNA binding to a target sequence results in either translational repression or a degrading of the target mRNA. To determine whether miR-378 down regulates CASP3 mRNA and/or protein, we analyzed CASP3 mRNA and protein expression in miR-378 expressing MC3T3-E1 cells cultured in hyper physiological glucose concentrations. Although CASP3 mRNA levels dropped significantly they were not as low as the knock down achieved by small hairpin RNA (shRNA) silencing of CASP3 (**Figure 3C**). In contrast, the drop in CASP3 protein levels was as strong as that achieved by shRNA silencing (**Figure 3D**).

Both caspase-3 depletion and ectopic MiR-378 expression counteract high glucose suppression of differentiation

To further explore the biological meaning of CASP3 down regulation by miR-378, we determined whether a depletion of CASP3 would ameliorate high glucose-suppressed osteoblast differentiation in the same way as achieved by ectopic miR-378 expression. Osteoblasts stably transfected with CASP3 shRNA (MC3-T3-E1/shCASP3) significantly increased ALP activity by the same amount attained by the overexpression of miR-378 (**Figure 3E**). An analysis of osteoblast specific gene expression revealed a similar trend. Whereas hyperglycemic conditions down regulated the expression of Runx2, Osx, Col I, OCN and ON, both CASP3 depletion and miR-378 expression restored the mRNA levels of osteogenic differentiation markers (**Figure 3F**).

Ectopic MiR-378 expression counteracts high glucose suppression of differentiation through activating the PI3K/Akt signaling pathway

To investigate whether miR-378 promotes osteoblast differentiation by PI3K and Akt signaling, we analyzed the expression levels of phosphorylated PI3K and Akt and found that ectopic miR-378 expression in MC3T3-E1 cells cultured in high glucose increases pPI3K and pAkt levels (**Figure 4A**). Furthermore, miR-378 overexpression decreased pro-apoptotic CytC, Apaf-1 and Bax protein levels (**Figure 4B**). This down regulation was inhibited by LY294002.

MiR-378 supresses CASP3 and regulates PI3K/Akt signaling pathway under hyperglycemic condition in vivo

Finally, the effect of miR-378 on CASP3 and PI3K/Akt signaling pathway was confirmed in diabetic mice model injected with miR-con or miR-378 plasmid. We found that the expression level of miR-378 was downregulated in HG group mice, and miR-378 plasmid injection restored its expression (**Figure 5A**). Meanwhile, ectopic miR-378 expression suppressed hyperglycemic condition induced the mRNA and protein expression level of miR-378 target CASP3 (**Figure 5B**). The levels of phosphorylated PI3K and Akt *in vivo*, which were consistent with that in high glucose cultured MC3T3-E1 cells, were downregulated under hyperglycemic condition compared to NG group mice, while ectopic miR-378 expression under hyperglycemic condition revered this effect (**Figure 5C**). In addition, miR-378 overexpression suppressed hyperglycemia-induced protein expressions of pro-apoptotic CASP3, CytC, Apaf-1 and Bax (**Figure 5D**).

Discussion

Here we show that the reduced osteogenic differentiation of osteoblast line MC3T3-E1 in high glucose media is accompanied by a down regulation of miR-378. When ectopically expressed, miR-378 restores osteoblast mineralization and viability in high glucose conditions. We show that this is likely to be due to the fact that apoptosis executer CASP3, a target of miR-378, promotes osteogenic differentiation. Both ectopic miR-378 expression and silencing of CASP3 restore ALP activity and the expression of markers of osteoblast differentiation. We further show that miR-378 activates the PI3K pathway and in doing so, reduces the levels of more pro-apoptotic proteins CytC, Apaf-1 and Bax. In addition, miR-378 negatively regulates CASP3 expression and activates the PI3K pathway, decreased pro-apoptotic proteins in diabetic model mice.

We confirm previous *in vitro* studies showing that high glucose concentrations decrease

osteoblast viability and differentiation capacity [5-8, 27, 45, 46]. It should be noted that the reduced mineralization caused by miR-378 could be caused by reduced cell numbers. In addition, whether reduced viability was caused by increased apoptosis or a slowing of the cell cycle was not investigated here.

Like a number of miRNAs, miR-378 has multiple targets, thereby eliciting different events in different cellular environments. Recently it was shown that miR-378 overexpression represses early osteoblast differentiation by silencing osteogenesis enhancer nephronectin, but enhances later stages of osteoblast differentiation because the binding to the nephronectin 3'UTR liberates another of its targets GalNT-7, an enzyme known to glycosylate proteins, including nephronectin [30], thereby allowing its secretion and promotion of osteogenesis. Therefore whether miR-378 functions in a pro- or anti-osteogenic capacity may depend on the presence and abundance of its targets. Our finding that ectopic miR-378 restores the differentiation and viability suppressed by hyper physiological glucose concentrations, opens up possibilities for further targets expressed within a cell reacting to high glucose. Since miR-378 also restored viability, apoptosis effector CASP3 was a logical candidate to investigate and we confirmed that CASP3 was a miR-378 target in a luciferase binding assay [33], and showed that miR-378 expression in osteoblasts reduced CASP3 mRNA and protein levels, indicating that in osteoblasts, too, miR-378 targets CASP3. Although we showed that miR-378 restores viability in osteoblasts and that it targets CASP3, it remains to be shown that miR-378 restores osteoblast viability specifically by targeting CASP3, for example by measuring apoptosis rates in cultures with or without stable miR-378 expression and co-expressing CASP3 with or without the seed region.

Culture in high glucose leads to the deregulation of osteogenic transcription factors, which underlies the defects in osteoblast maturation. We investigated whether a depletion of CASP3 amounted to the same relief of glucose induced transcriptional repression as an ectopic expression of miR-378 and found that both restored the expression of differentiation markers repressed by glucose. This indicates that improved survival (by CASP3 depletion) positively affects matrix mineralization. This could simply reflect the fact that improved survival increases the pool of cells available to undergo differentiation and create a mineralized matrix.

The molecular mechanism by which miR-378 activates the PI3K/Akt pathway is unknown. It is possible that miR-378 silences a gene which inhibits the PI3K/Akt pathway. However, the function of PI3K/Akt signaling in glucose induced suppression of differentiation and viability appears to be multifaceted. Zhang and Yang [47] previously showed that high glucose simultaneously suppressed osteogenic (but promoted adipogenic) differentiation by activating the PI3K/Akt pathway in primary rat osteoblasts. It is therefore curious that ectopic expression of osteogenesis promoting miR-378 under high glucose condition further activates the PI3K pathway yet restores osteogenesis.

High glucose condition appears to induce high levels of pro-apoptotic proteins CytC, Apaf-1 and Bax, which lie upstream of CASP3. MiR-378 expression reduced the levels of these pro-apoptotic proteins. This implies that miR-378 restores cell viability by two independent pathways, first by targeting CASP3 mRNA and second by reducing the levels of CytC, Apaf-1 and Bax. This might occur by miR-378 targeting of the individual proteins or an upstream activator.

We have revealed that high glucose culture of osteoblasts represses miR-378 and have shown that when ectopically expressed miR-378 counteracts the suppression of viability and differentiation caused by high glucose culture, and negatively regulates target gene CASP3 and activiates PI3K/Akt pathway both in high glucose cultured osteoblasts and diabetic model mice. Our results indicate that miR-378 restores viability and osteogenic differentiation by targeting CASP3 and inhibiting pro-apoptotic CytC, Apaf-1 and Bax proteins via the PI3K/Akt pathway. The positive effects of miR-378 on osteogenesis make it an interesting candidate to explore for therapeutic strategies.

Disclosure of conflict of interest

None.

Address correspondence to: Dr. Yongde Peng, Department of Endocrinology and Metabolism, Shanghai First People Hospital, Shanghai Jiao Tong University School of Medicine, 100 Haining Road,

Shanghai 200080, China. Tel: 86-21-63240090-5402; Fax: 86-21-63240090-5402, E-mail: pyongde@hotmail.com

References

[1] Blakytny R, Spraul M and Jude EB. Review: The diabetic bone: a cellular and molecular perspective. Int J Low Extrem Wounds 2011; 10: 16-32.

[2] Bouillon R. Diabetic bone disease. Calcif Tissue Int 1991; 49: 155-160.

[3] Rakel A, Sheehy O, Rahme E and LeLorier J. Osteoporosis among patients with type 1 and type 2 diabetes. Diabetes Metab 2008; 34: 193-205.

[4] Merlotti D, Gennari L, Dotta F, Lauro D and Nuti R. Mechanisms of impaired bone strength in type 1 and 2 diabetes. Nutr Metab Cardiovasc Dis 2010; 20: 683-690.

[5] Balint E, Szabo P, Marshall CF and Sprague SM. Glucose-induced inhibition of in vitro bone mineralization. Bone 2001; 28: 21-28.

[6] Dienelt A and zur Nieden NI. Hyperglycemia impairs skeletogenesis from embryonic stem cells by affecting osteoblast and osteoclast differentiation. Stem Cells Dev 2011; 20: 465-474.

[7] Kim HS, Park JW, Yeo SI, Choi BJ and Suh JY. Effects of high glucose on cellular activity of periodontal ligament cells in vitro. Diabetes Res Clin Pract 2006; 74: 41-47.

[8] Zhen D, Chen Y and Tang X. Metformin reverses the deleterious effects of high glucose on osteoblast function. J Diabetes Complications 2010; 24: 334-344.

[9] Garcia-Hernandez A, Arzate H, Gil-Chavarria I, Rojo R and Moreno-Fierros L. High glucose concentrations alter the biomineralization process in human osteoblastic cells. Bone 2012; 50: 276-288.

[10] Li YM, Schilling T, Benisch P, Zeck S, Meissner-Weigl J, Schneider D, Limbert C, Seufert J, Kassem M, Schutze N, Jakob F and Ebert R. Effects of high glucose on mesenchymal stem cell proliferation and differentiation. Biochem Biophys Res Commun 2007; 363: 209-215.

[11] Guntur AR, Rosen CJ and Naski MC. N-cadherin adherens junctions mediate osteogenesis through PI3K signaling. Bone 2012; 50: 54-62.

[12] Chiang C, Litingtung Y, Lee E, Young KE, Corden JL, Westphal H and Beachy PA. Cyclopia and defective axial patterning in mice lacking Sonic hedgehog gene function. Nature 1996; 383: 407-413.

[13] Nakamura T, Aikawa T, Iwamoto-Enomoto M, Iwamoto M, Higuchi Y, Pacifici M, Kinto N, Yamaguchi A, Noji S, Kurisu K and Matsuya T. In-

duction of osteogenic differentiation by hedgehog proteins. Biochem Biophys Res Commun 1997; 237: 465-469.

[14] Chen G, Deng C and Li YP. TGF-beta and BMP signaling in osteoblast differentiation and bone formation. Int J Biol Sci 2012; 8: 272-288.

[15] Lee MH, Kwon TG, Park HS, Wozney JM and Ryoo HM. BMP-2-induced Osterix expression is mediated by Dlx5 but is independent of Runx2. Biochem Biophys Res Commun 2003; 309: 689-694.

[16] Matsubara T, Kida K, Yamaguchi A, Hata K, Ichida F, Meguro H, Aburatani H, Nishimura R and Yoneda T. BMP2 regulates Osterix through Msx2 and Runx2 during osteoblast differentiation. J Biol Chem 2008; 283: 29119-29125.

[17] Yuasa T, Kataoka H, Kinto N, Iwamoto M, Enomoto-Iwamoto M, Iemura S, Ueno N, Shibata Y, Kurosawa H and Yamaguchi A. Sonic hedgehog is involved in osteoblast differentiation by cooperating with BMP-2. J Cell Physiol 2002; 193: 225-232.

[18] Day TF and Yang Y. Wnt and hedgehog signaling pathways in bone development. J Bone Joint Surg Am 2008; 90 Suppl 1: 19-24.

[19] Ortuno MJ, Ruiz-Gaspa S, Rodriguez-Carballo E, Susperregui AR, Bartrons R, Rosa JL and Ventura F. p38 regulates expression of osteoblast-specific genes by phosphorylation of osterix. J Biol Chem 2010; 285: 31985-31994.

[20] Ducy P, Zhang R, Geoffroy V, Ridall AL and Karsenty G. Osf2/Cbfa1: a transcriptional activator of osteoblast differentiation. Cell 1997; 89: 747-754.

[21] Nakashima K, Zhou X, Kunkel G, Zhang Z, Deng JM, Behringer RR and de Crombrugghe B. The novel zinc finger-containing transcription factor osterix is required for osteoblast differentiation and bone formation. Cell 2002; 108: 17-29.

[22] Neve A, Corrado A and Cantatore FP. Osteocalcin: skeletal and extra-skeletal effects. J Cell Physiol 2013; 228: 1149-1153.

[23] Termine JD, Kleinman HK, Whitson SW, Conn KM, McGarvey ML and Martin GR. Osteonectin, a bone-specific protein linking mineral to collagen. Cell 1981; 26: 99-105.

[24] Wang W, Zhang X, Zheng J and Yang J. High glucose stimulates adipogenic and inhibits osteogenic differentiation in MG-63 cells through cAMP/protein kinase A/extracellular signal-regulated kinase pathway. Mol Cell Biochem 2010; 338: 115-122.

[25] Lopez-Herradon A, Portal-Nunez S, Garcia-Martin A, Lozano D, Perez-Martinez FC, Cena V and Esbrit P. Inhibition of the canonical Wnt pathway by high glucose can be reversed by parathyroid hormone-related protein in osteo-

blastic cells. J Cell Biochem 2013; 114: 1908-1916.

[26] Zayzafoon M, Stell C, Irwin R and McCabe LR. Extracellular glucose influences osteoblast differentiation and c-Jun expression. J Cell Biochem 2000; 79: 301-310.

[27] Feng Z, Deng H, Du J, Chen D, Jiang R and Liang X. Lentiviral-mediated RNAi targeting p38MAPK ameliorates high glucose-induced apoptosis in osteoblast MC3T3-E1 cell line. Indian J Exp Biol 2011; 49: 94-104.

[28] Dong S, Yang B, Guo H and Kang F. MicroRNAs regulate osteogenesis and chondrogenesis. Biochem Biophys Res Commun 2012; 418: 587-591.

[29] Lian JB, Stein GS, van Wijnen AJ, Stein JL, Hassan MQ, Gaur T and Zhang Y. MicroRNA control of bone formation and homeostasis. Nat Rev Endocrinol 2012; 8: 212-227.

[30] Kahai S, Lee SC, Lee DY, Yang J, Li M, Wang CH, Jiang Z, Zhang Y, Peng C and Yang BB. MicroRNA miR-378 regulates nephronectin expression modulating osteoblast differentiation by targeting GalNT-7. PLoS One 2009; 4: e7535.

[31] Hupkes M, Sotoca AM, Hendriks JM, van Zoelen EJ and Dechering KJ. MicroRNA miR-378 promotes BMP2-induced osteogenic differentiation of mesenchymal progenitor cells. BMC Mol Biol 15: 1.

[32] Hua Z, Lv Q, Ye W, Wong CK, Cai G, Gu D, Ji Y, Zhao C, Wang J, Yang BB and Zhang Y. MiRNA-directed regulation of VEGF and other angiogenic factors under hypoxia. PLoS One 2006; 1: e116.

[33] Lee DY, Deng Z, Wang CH and Yang BB. MicroRNA-378 promotes cell survival, tumor growth, and angiogenesis by targeting SuFu and Fus-1 expression. Proc Natl Acad Sci U S A 2007; 104: 20350-20355.

[34] Fang J, Song XW, Tian J, Chen HY, Li DF, Wang JF, Ren AJ, Yuan WJ and Lin L. Overexpression of microRNA-378 attenuates ischemia-induced apoptosis by inhibiting caspase-3 expression in cardiac myocytes. Apoptosis 17: 410-423.

[35] Bachelder RE, Ribick MJ, Marchetti A, Falcioni R, Soddu S, Davis KR and Mercurio AM. p53 inhibits alpha 6 beta 4 integrin survival signaling by promoting the caspase 3-dependent cleavage of AKT/PKB. J Cell Biol 1999; 147: 1063-1072.

[36] Wang W, Olson D, Liang G, Franceschi RT, Li C, Wang B, Wang SS and Yang S. Collagen XXIV (Col24alpha1) promotes osteoblastic differentiation and mineralization through TGF-beta/Smads signaling pathway. Int J Biol Sci 2012; 8: 1310-1322.

[37] Gregory CA, Gunn WG, Peister A and Prockop DJ. An Alizarin red-based assay of mineralization by adherent cells in culture: comparison with cetylpyridinium chloride extraction. Anal Biochem 2004; 329: 77-84.

[38] Tietz NW, Burtis CA, Duncan P, Ervin K, Petitclerc CJ, Rinker AD, Shuey D and Zygowicz ER. A reference method for measurement of alkaline phosphatase activity in human serum. Clin Chem 1983; 29: 751-761.

[39] Chen C, Wang Y, Zhang J, Ma L, Gu J and Ho G. Contribution of neural cell death to depressive phenotypes of streptozotocin-induced diabetic mice. Dis Model Mech 2014; 7: 723-730.

[40] Yu W, Zha W, Guo S, Cheng H, Wu J and Liu C. Flos Puerariae Extract Prevents Myocardial Apoptosis via Attenuation Oxidative Stress in Streptozotocin-Induced Diabetic Mice. PLoS One 2014; 9: e98044.

[41] Jing D, Cai J, Shen G, Huang J, Li F, Li J, Lu L, Luo E and Xu Q. The preventive effects of pulsed electromagnetic fields on diabetic bone loss in streptozotocin-treated rats. Osteoporos Int 2011; 22: 1885-1895.

[42] Wang XT, Xie YB and Xiao Q. Lentivirus-mediated RNA interference targeting E2F-1 inhibits human gastric cancer MGC-803 cell growth in vivo. Exp Mol Med 2011; 43: 638-645.

[43] Tamura Y, Kawao N, Okada K, Yano M, Okumoto K, Matsuo O and Kaji H. Plasminogen activator inhibitor-1 is involved in streptozotocin-induced bone loss in female mice. Diabetes 2013; 62: 3170-3179.

[44] Botolin S and McCabe LR. Chronic hyperglycemia modulates osteoblast gene expression through osmotic and non-osmotic pathways. J Cell Biochem 2006; 99: 411-424.

[45] Alikhani M, Alikhani Z, Boyd C, MacLellan CM, Raptis M, Liu R, Pischon N, Trackman PC, Gerstenfeld L and Graves DT. Advanced glycation end products stimulate osteoblast apoptosis via the MAP kinase and cytosolic apoptotic pathways. Bone 2007; 40: 345-353.

[46] He H, Liu R, Desta T, Leone C, Gerstenfeld LC and Graves DT. Diabetes causes decreased osteoclastogenesis, reduced bone formation, and enhanced apoptosis of osteoblastic cells in bacteria stimulated bone loss. Endocrinology 2004; 145: 447-452.

[47] Zhang Y and Yang JH. Activation of the PI3K/Akt pathway by oxidative stress mediates high glucose-induced increase of adipogenic differentiation in primary rat osteoblasts. J Cell Biochem 2013; 114: 2595-2602.